Progress In Electromagnetics Research Letters, Vol. 100, 19–25, 2021

A Compact and Narrowband Displaced Substrate Integrated E-Plane Waveguide (SIEW) Junctions Filter

Danyang Huang[1, *], Xuan Hui Wu[2], and Qun Zhang[2]

Abstract—Substrate integrated E-plane waveguide (SIEW) was invented recently to design E-plane waveguide devices on printed circuit board, which cannot be achieved by using the conventional substrate integrated waveguide (SIW). This paper is the first time to present an E-plane displaced SIEW junctions bandpass filter. The proposed design is shorter than the recently published SIEW septa filter and has a smaller footprint than several other SIW filters. It is designed by mapping an equivalent E-plane waveguide filter to its SIEW implementation. A filter prototype is built and measured for validation.

1. INTRODUCTION

In modern wireless communications, researchers strive to design devices that are small, light weight, and can be highly integrated. Substrate integrated waveguide (SIW) is one of the techniques that achieve these benefits [1, 2]. Due to its compact size, low cost, and ease of integration, SIW has been extensively studied, and many SIW devices have been designed [3–8]. In particular, multilayer SIW is used to integrate circuits in the vertical direction by etching coupling slots on the shared waveguide walls between stacked SIWs. The utilized mode is the same as that in an SIW, with electric field perpendicular to the circuit board [9–11].

Although SIW and its multilayer version are successful to design an H-plane type of planar waveguide circuit with electric field perpendicular to the PCB in its utilized mode, they cannot be used to design an E-plane type of circuit whose electric field is parallel to the PCB. This issue has been resolved recently by the invention of substrate integrated E-plane waveguide (SIEW) [12]. In SIEW, two copper strips are inserted at the middle height and intersect all the through holes that emulate the vertical wall. The additional copper strips allow the longitudinal current flow [12, 13]. Since its invention, SIEW has been used to design an E-plane horn antenna and an array [14, 15], a dual linearly polarized horn antenna [13], and an SIEW adaptor that excites circular polarization [16].

The invention of SIEW antenna calls for the needs for SIEW filters because SIW filters are difficult to integrate with SIEW antennas. The first SIEW filter published in [13] was based on metallic septa. This type of design is normally longer than other filter types because the additional septa widths increase the filter length. An alternative technique for filter design is to create displaced junctions in the E-plane [17–21]. Each displaced junction forms a coupling window between neighboring waveguide sections. Since such coupling windows have zero lengths, they give shorter filter designs. This paper is the first time to report a displaced SIEW junctions filter. It has a smaller footprint than the existing SIEW septa filter and several other SIW filters.

Received 1 June 2021, Accepted 20 August 2021, Scheduled 7 September 2021

* Corresponding author: Danyang Huang (dhuang3@ncsu.edu).

[1] Department of Electrical and Computer Engineering, North Carolina State University Raleigh, North Carolina, USA. [2] Department of Electrical and Computer Engineering and Technology, Minnesota State University Mankato, Minnesota, USA.

2. SIEW FILTER DESIGN METHOD

The SIEW filter is designed by mapping a conventional displaced waveguide junctions filter into its SIEW implementation. It has a more compact size, lighter weight, and is easier for integration than the conventional metallic waveguide filter. Fig. 1(a) shows a third order E-plane displaced waveguide filter with three narrow-window-coupled waveguide resonators. The electrical field is parallel to the circuit plane. As seen, a displaced waveguide junction is created in the E-plane between every two neighbouring waveguide sections. These junctions are inductive, change the field distribution inside the waveguide, and make the circuit a shunt-inductance-coupled filter. Since the field distribution in the SIEW is similar to that in a conventional rectangular waveguide, the design method for a Butterworth type bandpass waveguide filter given in [22] can be used to design an SIEW filter. Fig. 1(b) shows the equivalent circuit of an nth order displaced waveguide junction filter, where Z_0 is the waveguide impedance; X_i with $1 \leq i \leq (n+1)$ is the equivalent reactance of the ith junction; and l_i with $1 \leq i \leq n$ is the length of the ith waveguide resonator. For the filter in Fig. 1(a), its equivalent circuit has $n = 3$ in Fig. 1(b). A higher filter order gives steeper rolloff as shown in Fig. 1(c).

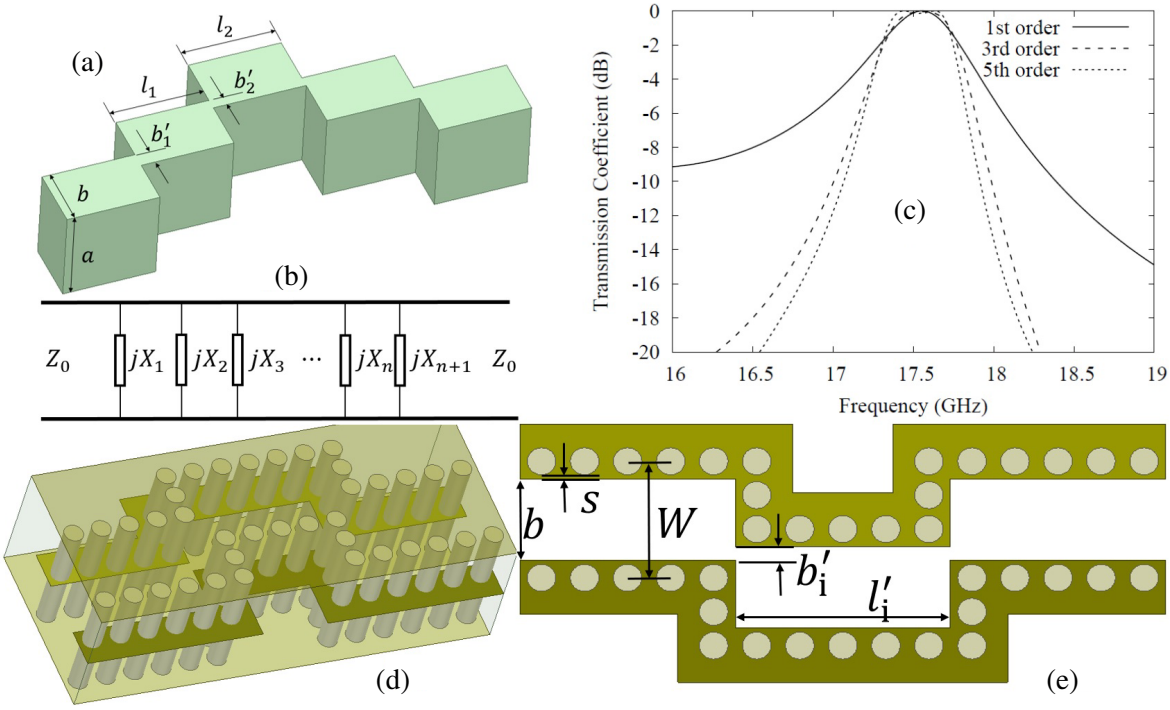

Figure 1. (a) A 3rd order symmetrical displaced waveguide junctions filter with three waveguide resonators and (b) the equivalent circuit of an nth order displaced waveguide junctions filter. (c) Filter responses with different orders. (d) The perspective view and (e) the middle layer layout of an SIEW resonator coupled with two SIEW sections.

For the design of a waveguide bandpass filter with the angular frequency band from ω_1 to ω_2, the ratio of X_i over Z_0 can be calculated as [22]

$$\frac{X_i}{Z_0} = \frac{K_i/Z_0}{1-(K_i/Z_0)^2} \tag{1}$$

where

$$\frac{K_i}{Z_0} = \begin{cases} \sqrt{\dfrac{\pi\omega_\lambda}{2g_{i-1}g_i}} & i = 1,\ (n+1) \\ \dfrac{\pi\omega_\lambda}{2\sqrt{g_{i-1}g_i}} & i = 2, 3, \cdots, n. \end{cases} \tag{2}$$

In Equation (2), g_i with $1 \leq i \leq (n+1)$ are the filter prototype parameters. For a third order filter, $g_0 = g_1 = g_3 = g_4 = 1$ and $g_2 = 2$ [22]. ω_λ in Equation (2) is the guided wavelength fractional bandwidth defined as

$$\omega_\lambda = \left(\frac{\lambda_{g_1} + \lambda_{g_2}}{2\lambda_0}\right)^2 \left(\frac{\omega_2 - \omega_1}{\omega_0}\right) \tag{3}$$

where λ_{g_1} and λ_{g_2} are the guided wavelengths at the cutoff frequencies ω_1 and ω_2, respectively, and λ_0 is the wavelength of a plane wave at the center frequency ω_0 defined as

$$\omega_0 = \sqrt{\omega_1 \omega_2}. \tag{4}$$

Given the value of X_i/Z_0 from Equation (1), the physical length of the waveguide resonator in Fig. 1(a) or Fig. 1(b) can be calculated as [22]

$$l_i = \frac{\lambda_{g_0}}{2\pi}\left[\pi - \frac{1}{2}\left(\tan^{-1}\frac{2X_i}{Z_0} + \tan^{-1}\frac{2X_{i+1}}{Z_0}\right)\right] \tag{5}$$

where $1 \leq i \leq n$ and λ_{g_0} is the guided wavelength at the center frequency ω_0. The ratio of the coupling window width over the waveguide width b'_i/b can be determined following the numerical calculation provided in [17]. For the waveguide filter in Fig. 1(a), the design is completed with the values of l_i and b'_i.

When the waveguide filter in Fig. 1(a) is implemented on the printed circuit board platform, the vertical metallic wall is realized using a sequence of copper plated through holes together with a copper strip that is inserted at the middle height. The through holes guide the vertical electrical current, and the copper strips guide longitudinal electrical current, both of which are required to design an E-plane waveguide circuit.

Figures 1(d) and (e) show the perspective view and the middle layer layout of an SIEW resonator that is coupled with two SIEW sections. The top and bottom surfaces of the device are entirely copper plated. When the waveguide filter in Fig. 1(a) is mapped into its SIEW implementation, the waveguide width b and coupling window width b'_i in Fig. 1(a) are used as the initial design values of the strip edge-to-edge spacings for the SIEW and SIEW coupling window in Fig. 1(e), respectively. However, the SIEW resonator length l'_i will be different from that of its waveguide counterpart because of their different guided wavelength values. It is obtained as

$$l'_i = l_i \frac{\lambda'_{g_0}}{\lambda_{g_0}} \tag{6}$$

where l_i is the waveguide resonator length from Eq. (5), and λ_{g_0} and λ'_{g_0} are the guided wavelengths of the waveguide resonator and the SIEW resonator, respectively, both at the center frequency. The values of λ_{g_0} and λ'_{g_0} can be obtained from Fig. 2.

An SIEW and its equivalent conventional waveguide counterpart are simulated to compare their guided wavelengths. Referring to Fig. 1(e), the SIEW has the through hole diameter of 1 mm, through hole period of 1.5 mm, copper strip edge-to-edge spacing of $b = 3$ mm, and the thickness of $a = 6.35$ mm. The strip insertion s is either 0.1 mm, 0.3 mm, or 0.5 mm. For fair comparison, the conventional waveguide has the same thickness of 6.35 mm and the width of 3 mm. The SIEW and waveguide use the same substrate with $\epsilon_r = 3.45$ and $\tan\delta = 0.002$. As seen in Fig. 2, the SIEW has a shorter guided wavelength than the conventional waveguide, so the SIEW resonator length l'_i in Fig. 1(e) will be less than the waveguide resonator l_i in Fig. 1(a). Moreover, at a lower frequency, the SIEW's guided wavelength depends on the value of the copper strip insertion s. The deeper the strip is inserted into the waveguide, the shorter the guided wavelength will be. However, at a higher frequency, such an effect can be ignored. It is because by increasing the s value, the SIEW's cutoff frequency will be reduced, which increases the propagation constant and thus reduces the guided wavelength. This also explains why such an s value effect is more observable when frequency gets closer to the cutoff frequency. At a center frequency of 17.5 GHz, the SIEW resonator length l'_i will be scaled from the waveguide resonator length l_i using a factor of 0.902 based on the results in Fig. 2. With the values of b'_i and l'_i determined for each SIEW resonator, an initial design of the SIEW filter is obtained. It will then be optimized using fullwave simulation to finalize the design.

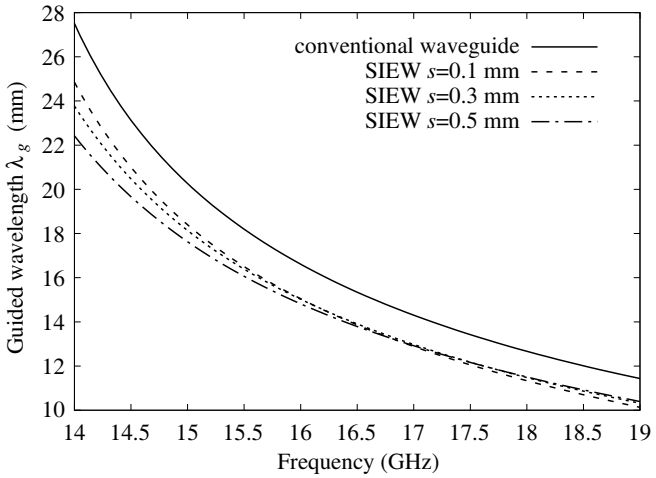

Figure 2. Guided wavelength comparison between the conventional waveguide and the SIEW with different s values.

3. SIMULATED AND MEASURED RESULTS

A displaced SIEW junctions filter is designed using the method presented in Section 2. Its perspective view and the three layouts on the top, middle, and bottom layers are shown in Fig. 3. The electric field distribution is also illustrated in Fig. 3(e). The filter is a symmetrical design with two SMA-to-SIEW transitions incorporated for measurement. The inner conductor of an SMA adapter is horizontally inserted into the SIEW at the middle height to excite horizontal electrical field. The vector electric field distributions with different excitation phases of 0°, 45°, 90°, and 135° are illustrated in Fig. 4. Those with excitation phases of 180°, 225°, 270°, and 315° are not shown because they are simply out of polarity of the 0°, 45°, 90°, and 135° cases, respectively. As seen, the excited electric fields in the SIEW are mainly horizontally directed. The T-shape copper sheet is for the soldering of the SMA inner conductor and also for impedance matching. The outer conductor of the SMA adaptor is soldered onto the copper strips that are on both sides of the T-shape strip. This design is based on Rogers TMM3 substrate with $\epsilon_{rx} = \epsilon_{ry} = 3.40$, $\epsilon_{rz} = 3.45$, and $\tan\delta_z = 0.002$. It is built by stacking and binding two

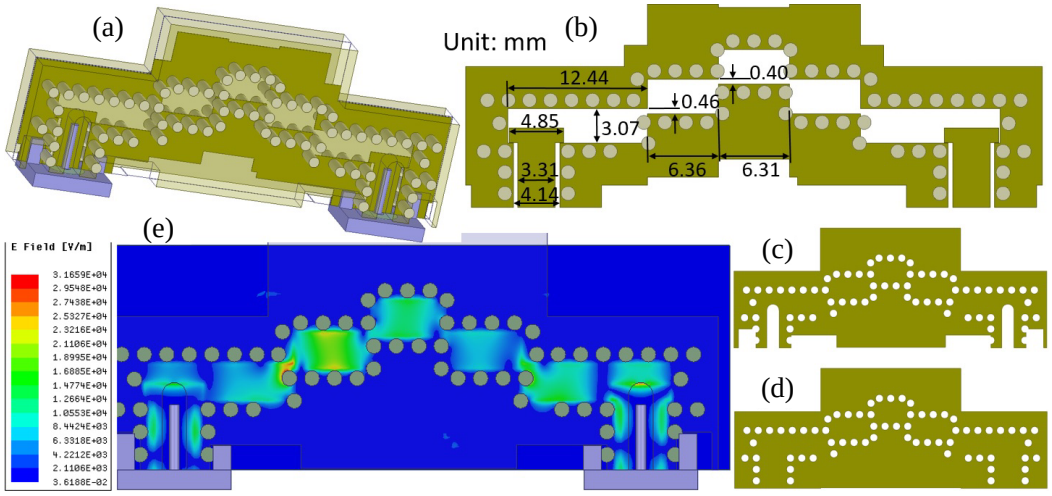

Figure 3. (a) The perspective view, (b) the middle layout, (c) the top layout, (d) the bottom layout and (e) the electric field distribution at 17.65 GHz of the displaced SIEW junctions filter.

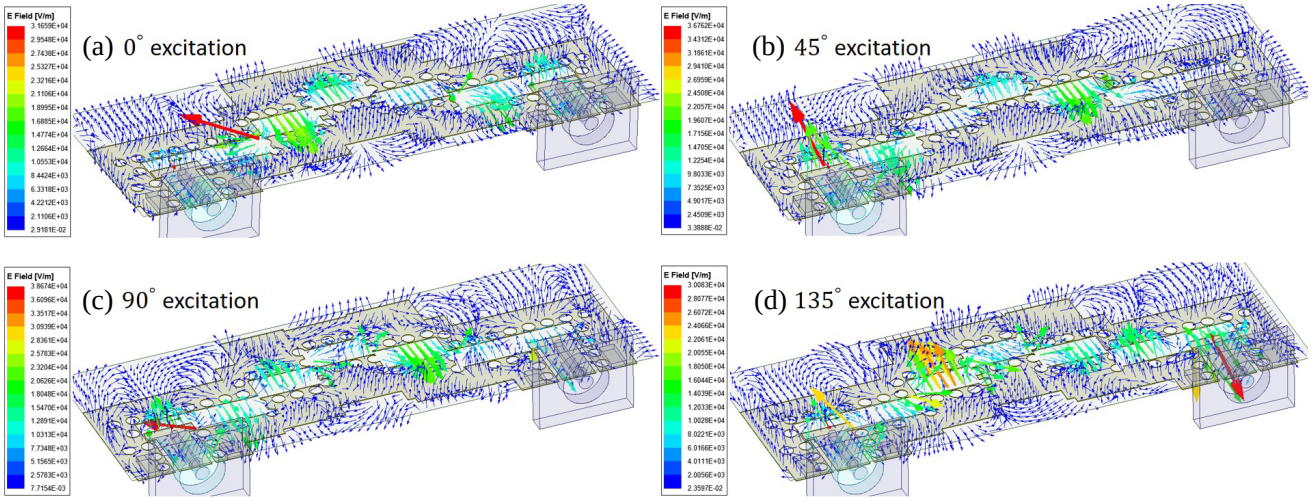

Figure 4. Vector electric field distribution at 17.65 GHz with (a) 0° excitation, (b) 45° excitation, (c) 90° excitation and (d) 135° excitation.

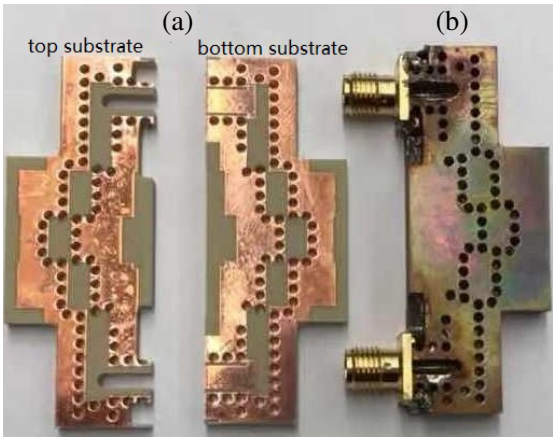

Figure 5. The SIEW filter prototype (a) before and (b) after assembling.

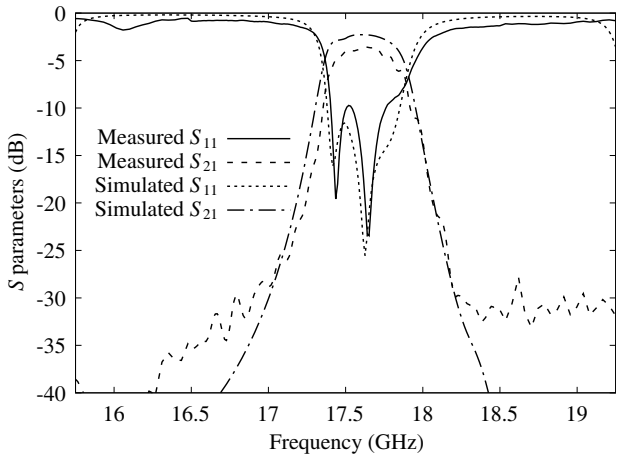

Figure 6. S parameters of the SIEW filter.

Rogers TMM3 substrates, each being 3.175 mm thick. Fig. 5 shows the SIEW filter prototype before and after assembling. In Fig. 5(a), the copper plating pattern on the bottom substrate is a mirrored image of that on the top substrate except that there are two additional 'T'-shape copper strips on the bottom substrate for the soldering of two SMA connectors' inner conductors. In addition, the top substrate has six cutouts to accommodate the inner and outer conductors of two SMA connectors. During assembling, a thin layer of solder is applied onto the shown copper layers in Fig. 5(a). Next, the two substrates are stacked face-to-face such that the copper patterns on the two substrates overlap. Then, the two substrates are bound together in a reflow oven. Lastly, two SMA connectors are soldered onto the bottom substrate.

The S parameters of the filter prototype is measured and compared to the simulated results in Fig. 6. The measured minimum insertion loss is 3.59 dB that is 1.4 dB higher than the simulated one. The measured 3 dB bandwidth is 500 MHz from 17.38 GHz to 17.88 GHz. The discrepancy between the simulated and measured results is mainly attributed to the imperfect alignment of the two substrates during assembling, the possible roughness of the substrate surface between the two substrates, and the undisclosed in-plane loss tangent value of the TMM3 substrate in data sheet.

Table 1. Filter comparison.

	this work	[13]	[5]	[6]	[7]	[8]
type	SIEW	SIEW	SIW	SIW	SIW	SIW
area (λ^2)	1.3	1.9	2.4	4.1	1.6	2.6
order	3	3	4	4	3	4
BW* (%)	2.8	3.3	9.9	3.4	6.5	3.7
f_c (GHz)	17.63	11.25	20.2	92.7	10.2	12.5
IL* (dB)	3.59	2.65	0.9	4.3	2.0	1.4

* BW: Bandwidth, IL: Insertion loss.

Table 1 compares several SIEW and SIW filters excluding the transition structures that are used for measurement purpose. A filter's size depends on the operating frequency and the choice of substrate. For fair comparison, the filter area data in Table 1 are normalized using λ^2 where λ is the wavelength in the substrate. As seen, the proposed filter has the best frequency selectivity with the narrowest bandwidth, while achieving the smallest footprint area. Particularly, the new design has a 31.6% size reduction and 15.2% bandwidth reduction compared to the SIEW septa filter [13]. The measured insertion loss is higher than most other filters in Table 1 except for the one in [6]. The insertion loss could be reduced by improving assembly tolerance to minimize substrate misalignment and solder layer unevenness. Adopting a different substrate with lower loss tangent value will also improve insertion loss.

4. CONCLUSIONS

A displaced SIEW junctions bandpass filter is presented. It is designed by mapping an equivalent E-plane displaced waveguide junctions filter onto the SIEW. It is demonstrated that SIEW has a shorter guided wavelength than its waveguide counterpart, so the filter size could be reduced. A filter prototype is built and measured for validation. Compared to the SIEW septa filter, the proposed filter has 31.6% size reduction and 15.2% bandwidth reduction that gives better frequency selectivity. It also has a smaller footprint and better frequency selectivity than several other SIW filters.

REFERENCES

1. Hirokawa, J. and M. Ando, "Single-layer feed waveguide consisting of posts for plane TEM wave excitation in parallel plates," *IEEE Transactions on Antennas and Propagation*, Vol. 46, No. 5, 625–630, May 1998.
2. Deslandes, D. and K. Wu, "Single-substrate integration technique of planar circuits and waveguide filters," *IEEE Transactions on Microwave Theory and Techniques*, Vol. 51, No. 2, 593–596, February 2003.
3. Xu, F. and K. Wu, "Guided-wave and leakage characteristics of substrate integrated waveguide," *IEEE Transactions on Microwave Theory and Techniques*, Vol. 53, No. 1, 66–73, January 2005.
4. Deslandes, D. and K. Wu, "Accurate modeling, wave mechanisms, and design considerations of a substrate integrated waveguide," *IEEE Transactions on Microwave Theory and Techniques*, Vol. 54, No. 6, 2516–2526, June 2006.
5. Chen, X.-P., K. Wu, and D. Drolet, "Substrate integrated waveguide filter with improved stopband performance for satellite ground terminal," *IEEE Transactions on Microwave Theory and Techniques*, Vol. 57, No. 3, 674–683, March 2009.
6. Xiao, Y., P. Shan, Y. Zhao, H. Sun, and F. Yang, "Design of a W-band GAAS-based SIW chip filter using higher order mode resonances," *IEEE Microwave and Wireless Components Letters*, Vol. 29, No. 2, 104–106, 2019.

7. Sun, L., H. Deng, Y. Xue, J. Zhu, and S. Xing, "Compact-balanced BPF and filtering crossover with intrinsic common-mode suppression using single-layered SIW cavity," *IEEE Microwave and Wireless Components Letters*, Vol. 30, No. 2, 144–147, 2020.
8. Liu, Q., D. Zhou, Y. Zhang, D. Zhang, and D. Lv, "Substrate integrated waveguide bandpass filters in box-like topology with bypass and direct couplings in diagonal cross-coupling path," *IEEE Transactions on Microwave Theory and Techniques*, Vol. 67, No. 3, 1014–1022, 2019.
9. Che, W., L. Xu, L. Geng, and D. Wang, "The propagation characteristics of double-layer substrate integrated waveguide (SIW) structure," *2006 Asia-Pacific Microwave Conference*, 1392–1394, 2006.
10. Abdel-Wahab, W. M. and S. Safavi-Naeini, "Low loss double-layer substrate integrated waveguide-hybrid branch line coupler for mm-wave antenna arrays," *2011 IEEE International Symposium on Antennas and Propagation (APSURSI)*, 2074–2076, 2011.
11. Luo, P., W. He, Y. Zhang, H. Liu, E. Forsberg, and S. He, "Leaky-wave antenna with wide scanning range based on double-layer substrate integrated waveguide," *IEEE Access*, Vol. 8, 199899–199908, 2020.
12. Huang, D., X. H. Wu, and Q. Zhang, "Concept of substrate integrated E-plane waveguide and waveguide filter," *2016 International Workshop on Antenna Technology (iWAT)*, 196–199, February 2016.
13. Hedin, M., D. Huang, X. H. Wu, and Q. Zhang, "Substrate integrated E-plane waveguide (SIEW) to design E-plane and dual polarized devices," *IEEE Transactions on Antennas and Propagation*, Vol. 67, No. 3, 1844–1853, March 2019.
14. Gu, Z., D. Huang, X. H. Wu, and Q. Zhang, "Substrate intergrated E-plane horn antenna," *Proc. IEEE Antennas Propag. Soc. Int. Symp.*, 1555–1556, June 2016.
15. Gu, Z., X. H. Wu, and Q. Zhang, "Substrate-integrated E-plane waveguide horn antenna and antenna array," *IEEE Transactions on Antennas and Propagation*, Vol. 66, No. 5, 2382–2391, May 2018.
16. Akunuru, V. N. K. R. and X. H. Wu, "Excitation of circularly polarized wave in substrate integrated E-plane waveguide," *Proc. IEEE Antennas Propag. Soc. Int. Symp.*, 1777–1778, 2019.
17. Kuhn, E., "Microwave bandpass filters consisting of rectangular waveguides with 1-dimensional offsets," *Int. J. Circ. Theor. App.*, Vol. 6, No. 1, 13–29, January 1978.
18. Sargent, G. A., "Reflection coefficients of offset rectangular waveguides at 56 GHz," *IEEE Transactions on Instrumentation and Measurement*, Vol. 23, No. 3, 246–247, September 1974.
19. Levy, R., "Reflection coefficient of unequal displaced rectangular waveguides (letters)," *IEEE Transactions on Microwave Theory and Techniques*, Vol. 24, No. 7, 480–483, July 1976.
20. Lerer, A. M., V. P. Lyapin, and G. P. Sinyavskii, "Displacements of rectangular waveguides," *Radiophys. Quantum Electron.*, Vol. 25, 671–678, January 1982.
21. Hunter, J. D., "The displaced rectangular waveguide junction and its use as an adjustable reference reflection," *IEEE Transactions on Microwave Theory and Techniques*, Vol. 32, No. 4, 387–394, April 1984.
22. Matthaei, G. L., L. Young, and E. M. T. Jones, *Microwave Filters, Impedance-matching Networks, and Coupling Structures*, Artech House Books, Artech House Microwave Library, 1980.